# Frustrated magnetic helices in MnSi-type crystals

Viacheslav A. Chizhikov\*, Vladimir E. Dmitrienko<sup>†</sup>

A.V. Shubnikov Institute of Crystallography, 119333 Moscow, Russia

The spiral magnetic order in cubic MnSi-type crystals is considered using the model of classical Heisenberg ferromagnetics with an extra interaction of the Dzyaloshinskii-Moriya (DM) type between neighboring atoms. For all shortest Mn-Mn bonds the DM vectors **D** are expressed via the **D**-vector for an arbitrary chosen bond, in accordance with the  $P2_13$  space group of these crystals and bond directions. The D-vectors have the same length and 24 different directions so that the components of the **D**-vectors are changing similarly to the components of the corresponding bond vectors. After minimization of the magnetic energy it is found how the wave vector  $\mathbf{k}$  of magnetic helices depends on **D**: for any helix direction  $k = 2(D_x - 2D_y - D_z)/(3J)$  where J is the exchange interaction constant and k-vector is in the units of the lattice constant. The wave number k determines both the sign and strength of global spiraling whereas locally, within a unit cell, the helical order can be strongly frustrated so that the twist angles between neighboring ferromagnetic layers may be even of different signs. Conical deformations of helices caused by an arbitrary directed external magnetic field is also considered within the same model. The critical field of helix unwinding is found and it is shown that even in the unwound state there remains a residual periodic splay of magnetic moments with the splay angle proportional to  $(D_x + D_z)/J$  which can be measured by diffraction methods. The third component of the **D**-vector,  $D_x + D_y - D_z$ , appears only in higher approximations. It is also demonstrated how the usually used continuous picture of moment distribution can be obtained from the discrete one in a coarse grain approximation.

PACS numbers: 75.25.-j, 75.10.Hk

# I. INTRODUCTION

The spiral arrangements appear in very different systems of condense matter physics and biology [1] providing an important example of a primitive self-organization. Sometimes this self-organization results in rather intricate structures (may be the first staircases to more complicated biological patterns) like the blue phases in chiral liquid crystals [2, 3] or the Skyrmion textures in chiral magnetics with B20 crystal structure (MnSi, MnGe, Fe<sub>1-x</sub>Co<sub>x</sub>Si) [4-6]. There is a remarkable similarity in the physics of those so different systems [7]. Therefore it is interesting and challenging to look for local interactions responsible for macroscopic spiral ordering and, in particular, to find relationships between parameters of the local interaction and the final structures. For instance, the first question is what determines the period and handedness of helices?

Most frequently, the helical arrangements are described phenomenologically, just by adding chiral terms like  $\mathcal{D}\mathbf{n}$  curl  $\mathbf{n}$  to the free energy of the system where vector  $\mathbf{n}(\mathbf{r})$  describes a local system anisotropy. The period and handedness of helices are determined by the absolute value and sign of the pseudoscalar coefficient  $\mathcal{D}$ ; of course this

<sup>\*</sup> email: chizhikov@crys.ras.ru

<sup>†</sup> email: dmitrien@crys.ras.ru

term should be allowed by the system symmetry (lack of inversion is required). In the chiral liquid crystals, the value of  $\mathcal{D}$  is believed to be determined by steric interactions between neighboring chiral molecules but any quantitative theory is still absent because of baffling complexity of the problem. In cubic magnetic crystals of the MnSi type, the helical ordering is induced by the Dzyaloshinskii–Moriya (DM) interaction between neighboring magnetic moments  $\mathbf{s}_i$  and  $\mathbf{s}_j$  [8, 9]. This interaction [10–13] can exist both in centrosymmetric and non-centrosymmetric crystals but only in the latter case it results in long-range helical structures. The most simple form of the DM term in the interaction energy is written as  $\mathbf{D}_{ij} \cdot [\mathbf{s}_i \times \mathbf{s}_j]$  where pseudovector coupling coefficients  $\mathbf{D}_{ij}$  originate from superexchange interaction via neighboring atoms.

It was shown by Moriya that vectors  $\mathbf{D}_{ij}$  are determined by asymmetry of local atomic arrangements. Recently it was carefully investigated, using synchrotron radiation and polarized neutron small-angle diffraction, what is the relationship between the handedness of the MnSi crystal structure and the sign of magnetic helix [14, 15]. It was unequivocally demonstrated that the structural chirality rigorously determines the magnetic chirality of these compounds. The interplay between structural chirality is also important for spin chirality in multilayer structures [16, 17]. However, no analytical formula related  $\mathcal{D}$  and  $\mathbf{D}_{ij}$  has been found yet even for the simple case of interaction between magnetic moments of neighboring atoms. This problem is indeed even more complicated because the itinerant nature of magnetism in MnSi crystals. Detailed numerical studies of the DM interaction in MnSi-type crystals are performed by Hopkinson and Kee [18] and their results will be discussed below in comparison with the results of the present paper.

A generic feature, intrinsic to complicated spacial structures, is frustration of their local ordering: the configurations with the best local energy cannot be spread for all the system. In the chiral liquid crystals and MnSi heliomagnetics, the most favorable double-twist local arrangements are restricted by topological constrains existing in two-dimensional and three-dimensional spaces [2, 3]. Nevertheless, the stable three-dimensional blue phases are possible in a narrow range of temperatures whereas the two-dimensional system of spin vertices can be stabilized by external magnetic field. However, in complicated crystals like La<sub>2</sub>CuO<sub>4</sub>, there is an additional mechanism of frustrations [19, 20] related with different orientations of  $\mathbf{D}_{ij}$  for different inter-spin bonds. We have found that this type of frustration is also intrinsic to the MnSi structure: at the atomic scale, spin rotation in the magnetic helices can be strongly nonmonotonic because of different orientations of  $\mathbf{D}_{ij}$  for different bonds. As a result, unequal righthand and lefthand twists usually coexist in each of the helices. For instance, the coefficient  $\mathcal{D}$  can become zero even for nonzero  $\mathbf{D}_{ij}$ .

In this paper we first find a simple analytical expression related the helix period and handedness with the DM vectors of the shortest Mn-Mn bonds. In this consideration, we adopt a usually used approximation that the exchange interaction is stronger than DM interaction and twist angles between neighboring atoms are correspondingly small. It is demonstrated that for general orientation of DM vectors the MnSi helical structure is frustrated so that the twist angles between neighboring ferromagnetic layers have different signs. Then, using the same approximations, conical distortions of helices in external magnetic fields are analyzed and the critical field of helix unwinding is determined. Finally, the parameters of the known phenomenological description of MnSi helices are related to the DM vectors of the microscopic theory.

#### II. MAGNETIC ENERGY AND CRYSTAL STRUCTURE

In a simple model of classical Heisenberg ferromagnetics with an extra interaction of the Dzyaloshinskii–Moriya (DM) type, the energy of the system is expressed as a sum of pair interactions between magnetic atoms and the interaction of individual atoms with an external magnetic field **H**:

$$E = \frac{1}{2} \sum_{i \neq j} (-J_{ij} \mathbf{s}_i \cdot \mathbf{s}_j + \mathbf{D}_{ij} \cdot [\mathbf{s}_i \times \mathbf{s}_j]) - g\mu_B \sum_i \mathbf{H} \cdot \mathbf{s}_i,$$
(1)

where the first summation is taken over all pairs  $\{ij\}$  of magnetic atoms,  $J_{ij}$  is the exchange interaction constant,  $\mathbf{D}_{ij}$  are the Dzyaloshinskii–Moriya vectors, and  $g\mu_B$  is an effective magnetic moment. Hereafter we will use the approximation of classical spins with ferromagnetic exchange coupling between nearest neighbors,  $J_{ij} \equiv J > 0$ , and suppose that  $|\mathbf{s}_i| = 1$  for all magnetic atoms. Using the nearest neighbor approximation for the MnSi-type crystals we can rewrite Eq. (1) as

$$E = \frac{1}{2} \sum_{i} \sum_{j=1}^{6} (-J \mathbf{s}_i \cdot \mathbf{s}_j + \mathbf{D}_{ij} \cdot [\mathbf{s}_i \times \mathbf{s}_j]) - g\mu_B \sum_{i} \mathbf{H} \cdot \mathbf{s}_i,$$
 (2)

where the first sum (i) is taken over all Mn atoms of the crystal and the second sum (j) is over six nearest Mn neighbors of i-th atom, i.e. over six bonds connecting each Mn atom with its nearest neighbors.

It should be emphasized that vectors  $\mathbf{D}_{ij}$  have different orientations for different bonds and relations between different  $\mathbf{D}_{ij}$  can be found from symmetry reasons. In the unit cell of MnSi-type crystals, the magnetic atoms are at the 4a positions with coordinates (x, x, x),  $(1 - x, \frac{1}{2} + x, \frac{1}{2} - x)$ ,  $(\frac{1}{2} - x, 1 - x, \frac{1}{2} + x)$ ,  $(\frac{1}{2} + x, \frac{1}{2} - x, 1 - x)$  [21]. There are 24 crystallographically equivalent bonds between nearest neighbors, and DM vectors for all bonds can be obtained from DM vector of any bond using symmetry transformations of the point group 23 of MnSi crystal augmented with the inversion; the latter appears owing to the permutation of atoms:  $\mathbf{D}_{ji} = -\mathbf{D}_{ij}$ . The procedure is, in principle, very simple: we choose an arbitrary vector  $(D_x, D_y, D_z)$  as DM vector of the "first" bond, say  $(-2x, \frac{1}{2}, \frac{1}{2} - 2x)$ , connecting Mn atom at (x, x, x) with Mn atom at  $(-x, \frac{1}{2} + x, \frac{1}{2} - x)$ . It should be an arbitrary vector because no symmetry operation is associated with the bond. Then, for this cubic space group, any shortest bond between Mn atoms can be obtained from the "first" one using cyclic permutations (i.e. threefold rotations) and/or sign inversions (i.e. twofold rotations and inversions) of its vector components. The components of the corresponding DM vector are expressed through  $D_x$ ,  $D_y$  and  $D_z$  by exactly the same cyclic permutations and/or sign inversions. The list of all the bonds and their  $\mathbf{D}$ -vectors is given in Table I. All  $\mathbf{D}_{ij}$  have the same length:  $|\mathbf{D}_{ij}| = D$ .

It was shown [19, 20] that the DM term should be accompanied by two extra terms:

$$E' = \frac{1}{2} \sum_{i \neq j} \left( \frac{\mathbf{D}_{ij}^2(\mathbf{s}_i \cdot \mathbf{s}_j)}{4J} - \frac{(\mathbf{s}_i \cdot \mathbf{D}_{ij})(\mathbf{D}_{ij} \cdot \mathbf{s}_j)}{2J} \right). \tag{3}$$

These terms are of the same order of magnitude as the DM term because for small DM interaction,  $|\mathbf{D}_{ij}| \ll J$ , small angles between  $\mathbf{s}_i$  and  $\mathbf{s}_j$  are of order  $|\mathbf{D}_{ij}|/J$ . In Eq. (3), with the same accuracy we can put  $\mathbf{s}_i = const$  for a small domain containing all 12 different interatomic bonds and averaging of  $(\mathbf{D}_{ij})_{\alpha}(\mathbf{D}_{ij})_{\beta}$  over these 12 bonds gives  $\frac{1}{3}D^2\delta_{\alpha\beta}$ . Thus Eq. (3) can be written as

$$E' = \frac{1}{2} \sum_{i \neq j} \frac{D^2}{12J} \mathbf{s}_i \cdot \mathbf{s}_j, \tag{4}$$

This term is isotropic and can be included into exchange term of Eq. (1). We see that in cubic crystals the extra terms given by Eq. (3) are not important if  $|\mathbf{D}_{ij}| \ll J$ .

Having a list of DM vectors one can calculate and minimize numerically the magnetic energies (1) and (2) for rather big sets of atoms with distinct moment configurations, including those similar to Skyrmions. However in this paper we will use only analytic calculations for detailed consideration of helical structures.

#### III. HELIX STRUCTURE IN THE ABSENCE OF MAGNETIC FIELD

Let us start with the simple case of free helices which provides a minimum of the magnetic energies (1) and (2) for  $\mathbf{H} = 0$ . As it is known from numerous experiments, well below the Curie point the magnetic moments of Mn atoms form a simple helix. However, in the general case, the helices may be different for four different types of equivalent atomic positions in the unit cell (i.e. for positions with four different orientations of the local threefold axes), and this is confirmed by numerical simulations. Then, the spin structure can be described by the superposition of four helices

$$\mathbf{s}^t = \mathbf{n}_{cos}^t \cos \mathbf{k} \cdot \mathbf{r} + \mathbf{n}_{sin}^t \sin \mathbf{k} \cdot \mathbf{r},\tag{5}$$

so that the condition  $|\mathbf{s}^t| = 1$  is obviously obeyed. Here  $\mathbf{r}$  is an atomic position,  $\mathbf{n}_{cos}^t$  and  $\mathbf{n}_{sin}^t$  are perpendicular unit vectors,  $\mathbf{k}$  is a wave vector. Upper index t = 1, 2, 3, 4 enumerates four atomic positions in the "first" unit cell: (x, x, x),  $(1 - x, \frac{1}{2} + x, \frac{1}{2} - x)$ ,  $(\frac{1}{2} - x, 1 - x, \frac{1}{2} + x)$ ,  $(\frac{1}{2} + x, \frac{1}{2} - x, 1 - x)$ , correspondingly. We express all the atomic positions in the units of the cubic unit cell so that both  $\mathbf{r}$  and  $\mathbf{k}$  vectors are dimensionless. Notice that all four spirals given by Eq. (5) have the same wave vector whereas in the Skyrmion-like structures there is a set of different wave vectors.

It can be easily seen that the spins of sublattice t rotate in the plane perpendicular to vector

$$\mathbf{n}_{rot}^t = [\mathbf{n}_{cos}^t \times \mathbf{n}_{sin}^t],\tag{6}$$

whose direction generally speaking can differ from that of wave vector  $\mathbf{k}$ .

Now, using Eq. (5) we can rewrite expression (2) for energy (at  $\mathbf{H} = 0$ ) as

$$E_{helix} = \frac{1}{2} \sum_{i} \sum_{j=1}^{6} \left\{ \left( -J \mathbf{n}_{cos}^{t(i)} \cdot \mathbf{n}_{cos}^{t(j)} + \mathbf{D}_{ij} \cdot [\mathbf{n}_{cos}^{t(i)} \times \mathbf{n}_{cos}^{t(j)}] \right) \cos \mathbf{k} \cdot \mathbf{r}_{i} \cos \mathbf{k} \cdot \mathbf{r}_{j} \right.$$

$$\left. + \left( -J \mathbf{n}_{cos}^{t(i)} \cdot \mathbf{n}_{sin}^{t(j)} + \mathbf{D}_{ij} \cdot [\mathbf{n}_{cos}^{t(i)} \times \mathbf{n}_{sin}^{t(j)}] \right) \cos \mathbf{k} \cdot \mathbf{r}_{i} \sin \mathbf{k} \cdot \mathbf{r}_{j} \right.$$

$$\left. + \left( -J \mathbf{n}_{sin}^{t(i)} \cdot \mathbf{n}_{cos}^{t(j)} + \mathbf{D}_{ij} \cdot [\mathbf{n}_{sin}^{t(i)} \times \mathbf{n}_{cos}^{t(j)}] \right) \sin \mathbf{k} \cdot \mathbf{r}_{i} \cos \mathbf{k} \cdot \mathbf{r}_{j} \right.$$

$$\left. + \left( -J \mathbf{n}_{sin}^{t(i)} \cdot \mathbf{n}_{sin}^{t(j)} + \mathbf{D}_{ij} \cdot [\mathbf{n}_{sin}^{t(i)} \times \mathbf{n}_{sin}^{t(j)}] \right) \sin \mathbf{k} \cdot \mathbf{r}_{i} \sin \mathbf{k} \cdot \mathbf{r}_{j} \right\},$$

$$(7)$$

where upper index t(i) designates "type" of *i*-th atom or its belonging to one of four sublattices,  $t(i) = 1 \dots 4$ . The sines and cosines products in Eq. (7) can be expressed through sines and cosines of arguments  $\mathbf{k} \cdot (2\mathbf{r}_i + \mathbf{r}_{ij})$  and  $\mathbf{k} \cdot \mathbf{r}_{ij}$ , with  $\mathbf{r}_{ij}$  being the distance between *i*-th and *j*-th atoms,  $\mathbf{r}_{ij} = \mathbf{r}_j - \mathbf{r}_i$ . It should be noted here that dependence on atomic positions is present in these trigonometric functions only. After summation over all unit cells of the crystal all the functions of argument  $\mathbf{k} \cdot (2\mathbf{r}_i + \mathbf{r}_{ij})$  vanish because  $\mathbf{k}$  is not a reciprocal lattice vector, whereas the functions of argument  $\mathbf{k} \cdot \mathbf{r}_{ij}$  do not depend on the unit cells to which *i*-th and *j*-th atoms belong. Thus we can rewrite expression

(7) for energy as

$$E_{helix} = \frac{N_{cell}}{4} \sum_{i=1}^{4} \sum_{j=1}^{6} \{ (-J\mathbf{n}_{cos}^{i} \cdot \mathbf{n}_{cos}^{t(j)} + \mathbf{D}_{ij} \cdot [\mathbf{n}_{cos}^{i} \times \mathbf{n}_{cos}^{t(j)}]) \cos \mathbf{k} \cdot \mathbf{r}_{ij}$$

$$+ (-J\mathbf{n}_{cos}^{i} \cdot \mathbf{n}_{sin}^{t(j)} + \mathbf{D}_{ij} \cdot [\mathbf{n}_{cos}^{i} \times \mathbf{n}_{sin}^{t(j)}]) \sin \mathbf{k} \cdot \mathbf{r}_{ij}$$

$$- (-J\mathbf{n}_{sin}^{i} \cdot \mathbf{n}_{cos}^{t(j)} + \mathbf{D}_{ij} \cdot [\mathbf{n}_{sin}^{i} \times \mathbf{n}_{cos}^{t(j)}]) \sin \mathbf{k} \cdot \mathbf{r}_{ij}$$

$$+ (-J\mathbf{n}_{sin}^{i} \cdot \mathbf{n}_{sin}^{t(j)} + \mathbf{D}_{ij} \cdot [\mathbf{n}_{sin}^{i} \times \mathbf{n}_{sin}^{t(j)}]) \cos \mathbf{k} \cdot \mathbf{r}_{ij} \},$$

$$(8)$$

where  $N_{cell}$  is the number of unit cells in the crystal, and first sum is now taken over four magnetic atoms within one unit cell, so t(i) = i.

Eq. (8) seems to be simple enough for possible minimization. It depends on 15 variables only: three angles characterizing orientation of triad  $\{\mathbf{n}_{cos}^t, \mathbf{n}_{sin}^t, \mathbf{n}_{rot}^t\}$  for each of four Mn sublattices, and three components of the wave vector  $\mathbf{k}$ . The exchange interaction constant J, DM vectors  $\mathbf{D}_{ij}$  and distances  $\mathbf{r}_{ij}$  between neighboring atoms are supposed to be invariable; we do not consider phenomena (e.g. magnetostriction) changing these parameters. Below, instead of numerical minimization, we will look for approximate analytical solutions relying on a small parameter.

Indeed, it is known from the experimental data that the spin-orbit interaction is usually much smaller than the exchange one, so that  $|\mathbf{D}_{ij}| \ll J$ . In the MnSi crystal, strong exchange interaction leads to the ferromagnetic ordering, whereas small DM interaction results in small canting of neighboring magnetic moments. Small values of D/J and  $|\mathbf{k}|$  (the latter is supposed to be of the order of D/J) allows us to perform approximate minimization of the energy. In particular, we can take advantage of the fact, that in this approximation the triads  $\{\mathbf{n}_{cos}^t, \mathbf{n}_{sin}^t, \mathbf{n}_{rot}^t\}$  have close orientations for four Mn sublattices.

Let us suppose that all triads  $\{\mathbf{n}_{cos}^t, \mathbf{n}_{sin}^t, \mathbf{n}_{rot}^t\}$  are close to triad  $\{\mathbf{n}_1, \mathbf{n}_2, \mathbf{n}_3\}$ , with  $\mathbf{n}_3$  being a vector, which can differ from  $\mathbf{n}_{\mathbf{k}} = \mathbf{k}/k$  ( $k = \pm |\mathbf{k}|$  is a wave number; the sign defines the chirality of the helix), and  $\{\mathbf{n}_1, \mathbf{n}_2\}$  being an orthonormal basis of the plane perpendicular to  $\mathbf{n}_3$ ,  $[\mathbf{n}_1 \times \mathbf{n}_2] = \mathbf{n}_3$ . It is useful to introduce vector  $\mathbf{n}_3 \neq \mathbf{n}_{\mathbf{k}}$  for considering all partial helices on an equal footing and for possible future consideration of anisotropy effects.

The deviation of triad  $\{\mathbf{n}_{cos}^t, \mathbf{n}_{sin}^t, \mathbf{n}_{rot}^t\}$  from  $\{\mathbf{n}_1, \mathbf{n}_2, \mathbf{n}_3\}$  can be considered as a sum of two small rotations: first one on the axis  $\mathbf{n}_3$  by the angle  $\omega_t$ , and another one by the angle  $\vec{\gamma}_t \perp \mathbf{n}_3$ . Then, the vectors  $\mathbf{n}_{cos}^t$ ,  $\mathbf{n}_{sin}^t$ , and  $\mathbf{n}_{rot}^t$  can be represented as

$$\begin{cases}
\mathbf{n}_{cos}^{t} = (R^{t}\mathbf{n}_{1})\cos\omega_{t} + (R^{t}\mathbf{n}_{2})\sin\omega_{t}, \\
\mathbf{n}_{sin}^{t} = -(R^{t}\mathbf{n}_{1})\sin\omega_{t} + (R^{t}\mathbf{n}_{2})\cos\omega_{t}, \\
\mathbf{n}_{rot}^{t} = R^{t}\mathbf{n}_{3},
\end{cases} \tag{9}$$

with  $R^t \equiv R(\vec{\gamma}_t)$  being the rotation matrix by the angle  $\vec{\gamma}_t$ . The substitution of Eq. (9) into Eq. (8) gives

$$E_{helix} = \frac{N_{cell}}{4} \sum_{i=1}^{4} \sum_{j=1}^{6} \left\{ -J\{(R^{i}\mathbf{n}_{1}) \cdot (R^{t(j)}\mathbf{n}_{1}) + (R^{i}\mathbf{n}_{2}) \cdot (R^{t(j)}\mathbf{n}_{2})\} \cos(\omega_{i} - \omega_{t(j)} - \mathbf{k} \cdot \mathbf{r}_{ij}) \right.$$

$$\left. -J\{(R^{i}\mathbf{n}_{2}) \cdot (R^{t(j)}\mathbf{n}_{1}) - (R^{i}\mathbf{n}_{1}) \cdot (R^{t(j)}\mathbf{n}_{2})\} \sin(\omega_{i} - \omega_{t(j)} - \mathbf{k} \cdot \mathbf{r}_{ij}) \right.$$

$$\left. +\mathbf{D}_{ij} \cdot \{[(R^{i}\mathbf{n}_{1}) \times (R^{t(j)}\mathbf{n}_{1})] + [(R^{i}\mathbf{n}_{2}) \times (R^{t(j)}\mathbf{n}_{2})]\} \cos(\omega_{i} - \omega_{t(j)} - \mathbf{k} \cdot \mathbf{r}_{ij}) \right.$$

$$\left. +\mathbf{D}_{ij} \cdot \{[(R^{i}\mathbf{n}_{2}) \times (R^{t(j)}\mathbf{n}_{1})] - [(R^{i}\mathbf{n}_{1}) \times (R^{t(j)}\mathbf{n}_{2})]\} \sin(\omega_{i} - \omega_{t(j)} - \mathbf{k} \cdot \mathbf{r}_{ij}) \right\}.$$

$$(10)$$

The seeming dependence on arbitrary vectors  $\mathbf{n}_1$  and  $\mathbf{n}_2$  can be eliminated with use of following two equations

$$(\mathbf{n}_1)_{\alpha}(\mathbf{n}_1)_{\beta} + (\mathbf{n}_2)_{\alpha}(\mathbf{n}_2)_{\beta} = \delta_{\alpha\beta} - (\mathbf{n}_3)_{\alpha}(\mathbf{n}_3)_{\beta}, \tag{11a}$$

$$(\mathbf{n}_2)_{\alpha}(\mathbf{n}_1)_{\beta} - (\mathbf{n}_1)_{\alpha}(\mathbf{n}_2)_{\beta} = -\varepsilon_{\alpha\beta\gamma}(\mathbf{n}_3)_{\gamma}. \tag{11b}$$

Then,

$$E_{helix} = \frac{N_{cell}}{4} \sum_{i=1}^{4} \sum_{j=1}^{6} \{-JR_{\alpha\mu}^{i} R_{\alpha\nu}^{t(j)} (\delta_{\mu\nu} - (\mathbf{n}_{3})_{\mu} (\mathbf{n}_{3})_{\nu}) \cos(\omega_{i} - \omega_{t(j)} - \mathbf{k} \cdot \mathbf{r}_{ij})$$

$$+JR_{\alpha\mu}^{i} R_{\alpha\nu}^{t(j)} \varepsilon_{\mu\nu\sigma} (\mathbf{n}_{3})_{\sigma} \sin(\omega_{i} - \omega_{t(j)} - \mathbf{k} \cdot \mathbf{r}_{ij})$$

$$+(\mathbf{D}_{ij})_{\alpha} \varepsilon_{\alpha\beta\lambda} R_{\beta\mu}^{i} R_{\lambda\nu}^{t(j)} (\delta_{\mu\nu} - (\mathbf{n}_{3})_{\mu} (\mathbf{n}_{3})_{\nu}) \cos(\omega_{i} - \omega_{t(j)} - \mathbf{k} \cdot \mathbf{r}_{ij})$$

$$-(\mathbf{D}_{ij})_{\alpha} \varepsilon_{\alpha\beta\lambda} R_{\beta\mu}^{i} R_{\lambda\nu}^{t(j)} \varepsilon_{\mu\nu\sigma} (\mathbf{n}_{3})_{\sigma} \sin(\omega_{i} - \omega_{t(j)} - \mathbf{k} \cdot \mathbf{r}_{ij}) \}.$$

$$(12)$$

The phases  $\omega$  are presented in expression (12) only as differences, which is in agreement with the fact, that they are defined up to a constant term associated with the origin choice. The matrix  $R(\vec{\gamma})$  can be expressed through the coordinates of the vector  $\vec{\gamma}$ :

$$(R(\vec{\gamma}))_{\alpha\beta} = \cos \gamma \delta_{\alpha\beta} - \frac{\sin \gamma}{\gamma} \varepsilon_{\alpha\beta\sigma} \gamma_{\sigma} + \frac{1 - \cos \gamma}{\gamma^2} \gamma_{\alpha} \gamma_{\beta} \approx \delta_{\alpha\beta} - \varepsilon_{\alpha\beta\sigma} \gamma_{\sigma} + \frac{1}{2} (\gamma_{\alpha} \gamma_{\beta} - \delta_{\alpha\beta} \gamma^2),$$
(13)

with  $\gamma = |\vec{\gamma}|$ . Then, we can rewrite the energy up to second order terms on  $|\mathbf{k}| \sim (\omega_i - \omega_{t(j)}) \sim \gamma \sim (D/J)$ :

$$E_{helix} = N_{cell}(-12J + \epsilon_1 + \epsilon_2), \tag{14}$$

with

$$\epsilon_1 = \frac{1}{2} \sum_{i=1}^4 \sum_{j=1}^6 \left\{ \frac{J}{2} (\omega_i - \omega_{t(j)} - \mathbf{k} \cdot \mathbf{r}_{ij})^2 - (\mathbf{D}_{ij} \cdot \mathbf{n}_3)(\omega_i - \omega_{t(j)} - \mathbf{k} \cdot \mathbf{r}_{ij}) \right\},\tag{15}$$

$$\epsilon_2 = \frac{1}{4} \sum_{i=1}^4 \sum_{j=1}^6 \left\{ \frac{J}{2} (\vec{\gamma}_i - \vec{\gamma}_{t(j)})^2 - \mathbf{D}_{ij} \cdot (\vec{\gamma}_i - \vec{\gamma}_{t(j)}) \right\}. \tag{16}$$

As we can see, the energy breaks up into two contributions depending on  $\omega$  and  $\vec{\gamma}$  and related to each other only by direction of the axis  $\mathbf{n}_3$ .

The routine minimization of  $\epsilon_1$  as a function of independent variables  $(\omega_2 - \omega_1)$ ,  $(\omega_3 - \omega_1)$  and  $(\omega_4 - \omega_1)$  (performed with Wolfram Research Mathematica) gives

$$\begin{cases}
\omega_{2} - \omega_{1} = -\frac{1}{4}(k_{x} + k_{z})(1 - 8x) - \frac{D_{x} + D_{z}}{2J}((\mathbf{n}_{3})_{x} + (\mathbf{n}_{3})_{z}), \\
\omega_{3} - \omega_{1} = -\frac{1}{4}(k_{x} + k_{y})(1 - 8x) - \frac{D_{x} + D_{z}}{2J}((\mathbf{n}_{3})_{x} + (\mathbf{n}_{3})_{y}), \\
\omega_{4} - \omega_{1} = -\frac{1}{4}(k_{y} + k_{z})(1 - 8x) - \frac{D_{x} + D_{z}}{2J}((\mathbf{n}_{3})_{y} + (\mathbf{n}_{3})_{z}),
\end{cases} (17)$$

and

$$\epsilon_1 = J \left( -\frac{(D_x + D_z)^2}{J^2} + \frac{3}{4}k^2 - k\frac{D_x - 2D_y - D_z}{J} (\mathbf{n_k} \cdot \mathbf{n_3}) \right).$$
 (18)

It is natural that  $\epsilon_1$  does not depend on x, because real atomic coordinates are not involved in energy definition (1). From the physical point of view it is more interesting that  $\epsilon_1$  is also independent of orientation of wave vector  $\mathbf{k}$  relative to coordinate axes. This fact is in a good accordance with experimental evidence of the possibility of easy reorientation of helix axis in MnSi by magnetic field, surface anchoring or other effects.

The minimization of the expression (18) on k gives us the following value for the wave number depending on DM vector  $\mathbf{D}$  and rotation axis orientation relative to  $\mathbf{k}$ 

$$k(\mathbf{D}, \widehat{\mathbf{n_k} \mathbf{n_3}}) = \frac{2}{3} \left( \frac{D_x - 2D_y - D_z}{J} \right) (\mathbf{n_k} \cdot \mathbf{n_3}), \tag{19}$$

and the part  $\epsilon_1$  of unit cell magnetic energy can be finally expressed as

$$\epsilon_1 = J \left( -\frac{(D_x + D_z)^2}{J^2} - \frac{1}{3} \frac{(D_x - 2D_y - D_z)^2}{J^2} (\mathbf{n_k} \cdot \mathbf{n_3})^2 + \frac{3}{4} (k - k(\mathbf{D}, \widehat{\mathbf{n_k n_3}}))^2 \right), \tag{20}$$

thereby the elasticity of the helix is  $\frac{3}{4}J$ .

It is evident from Eq. (20) that  $\epsilon_1$  has minimum, when  $\mathbf{n}_3$  coincides with  $\mathbf{n}_k$ , but it should be noted that, when  $\mathbf{n}_3$  deviates from  $\mathbf{n}_k$  by a small angle  $\gamma \sim (D/J)$ , the energy obtains only a small positive addition of the order of  $J(D/J)^4$ . Thus, there is a soft mode associated with deviation of rotation axis from helix direction. This deviation gives a cycloidal component to the helix.

Eq. (16) for  $\epsilon_2$  contains vectors  $\vec{\gamma}_t$  only within differences, so, in analogy with  $\omega$ , the vectors  $\vec{\gamma}_t$  are defined up to a constant vector perpendicular to  $\mathbf{n}_3$ . However, unlike the case of  $\omega$ , where a common term added to all phases results only in redefining of the origin, the constant vector added to all vectors  $\vec{\gamma}_t$  turns rotation axes for all four sublattices by the same angle. In fact, this turning has been already taken into account in the dependence of  $\epsilon_1$  on  $(\mathbf{n}_k \cdot \mathbf{n}_3)$ . We should also remind that Eq. (16) has been obtained in the assumption that  $\gamma \sim (D/J)$ . In order to avoid the ambiguity of definition of vectors  $\vec{\gamma}_t$ , we can use additional condition  $\sum_{t=1}^4 \vec{\gamma}_t = 0$ .

The routine minimization of  $\epsilon_2$  on independent variables  $(\vec{\gamma}_2 - \vec{\gamma}_1)$ ,  $(\vec{\gamma}_3 - \vec{\gamma}_1)$  and  $(\vec{\gamma}_4 - \vec{\gamma}_1)$  (performed with Wolfram Research Mathematica) gives

$$\begin{cases}
\vec{\gamma}_{2} - \vec{\gamma}_{1} &= \frac{D_{x} + D_{z}}{2J} \{ (\mathbf{n}_{3})_{x} (\mathbf{n}_{3})_{z} - (\mathbf{n}_{3})_{y}^{2} - (\mathbf{n}_{3})_{z}^{2}, \\
 &\quad (\mathbf{n}_{3})_{x} (\mathbf{n}_{3})_{y} + (\mathbf{n}_{3})_{y} (\mathbf{n}_{3})_{z}, (\mathbf{n}_{3})_{x} (\mathbf{n}_{3})_{z} - (\mathbf{n}_{3})_{x}^{2} - (\mathbf{n}_{3})_{y}^{2} \}, \\
\vec{\gamma}_{3} - \vec{\gamma}_{1} &= \frac{D_{x} + D_{z}}{2J} \{ (\mathbf{n}_{3})_{x} (\mathbf{n}_{3})_{y} - (\mathbf{n}_{3})_{y}^{2} - (\mathbf{n}_{3})_{z}^{2}, \\
 &\quad (\mathbf{n}_{3})_{x} (\mathbf{n}_{3})_{y} - (\mathbf{n}_{3})_{x}^{2} - (\mathbf{n}_{3})_{z}^{2}, (\mathbf{n}_{3})_{x} (\mathbf{n}_{3})_{z} + (\mathbf{n}_{3})_{y} (\mathbf{n}_{3})_{z} \}, \\
\vec{\gamma}_{4} - \vec{\gamma}_{1} &= \frac{D_{x} + D_{z}}{2J} \{ (\mathbf{n}_{3})_{x} (\mathbf{n}_{3})_{y} + (\mathbf{n}_{3})_{x} (\mathbf{n}_{3})_{z}, \\
 &\quad (\mathbf{n}_{3})_{y} (\mathbf{n}_{3})_{z} - (\mathbf{n}_{3})_{x}^{2} - (\mathbf{n}_{3})_{z}^{2}, (\mathbf{n}_{3})_{y} (\mathbf{n}_{3})_{z} - (\mathbf{n}_{3})_{y}^{2} \},
\end{cases} (21)$$

and

$$\epsilon_2 = -\frac{(D_x + D_z)^2}{J}. (22)$$

The full energy of the helix can be now written as

$$E_{helix} = N_{cell} J \left( -12 - 2 \frac{(D_x + D_z)^2}{J^2} - \frac{1}{3} \frac{(D_x - 2D_y - D_z)^2}{J^2} (\mathbf{n_k} \cdot \mathbf{n_3})^2 + \frac{3}{4} (k - k(\mathbf{D}, \widehat{\mathbf{n_k}\mathbf{n_3}}))^2 \right), \tag{23}$$

where the contribution -12J per unit cell is associated with ferromagnetic ordering of spins (12 is the number of Mn-Mn bonds per unit cell), the term  $-2\frac{(D_x+D_z)^2}{J}$ , combining  $\epsilon_2$  with a part of  $\epsilon_1$ , describes the energy of divergence between sublattices (the energy of canting), and remaining terms represent the twist energy of the helix.

The minimum of the energy (23) is achieved, when  $\mathbf{n}_3 = \mathbf{n}_k$ . Then,

$$E_{helix} = N_{cell}J\left(-12 - 2\frac{(D_x + D_z)^2}{J^2} - \frac{1}{3}\frac{(D_x - 2D_y - D_z)^2}{J^2} + \frac{3}{4}(k - k(\mathbf{D}))^2\right),\tag{24}$$

where

$$k(\mathbf{D}) = \frac{2}{3} \left( \frac{D_x - 2D_y - D_z}{J} \right). \tag{25}$$

It is also useful to write the full divergence vectors for sublattices using the formula

$$\vec{\psi} = \omega \mathbf{n}_3 + \vec{\gamma}. \tag{26}$$

then, from Eqs. (17) and (21) follows

$$\begin{cases}
\vec{\psi}_{2} - \vec{\psi}_{1} = \frac{\sqrt{3}}{4} \frac{D_{x} + D_{z}}{J} (\mathbf{e}_{2} - \mathbf{e}_{1}) + \frac{\sqrt{3}}{8} (1 - 8x) (\mathbf{k} \cdot \mathbf{e}_{2} - \mathbf{k} \cdot \mathbf{e}_{1}) \mathbf{n}_{3}, \\
\vec{\psi}_{3} - \vec{\psi}_{1} = \frac{\sqrt{3}}{4} \frac{D_{x} + D_{z}}{J} (\mathbf{e}_{3} - \mathbf{e}_{1}) + \frac{\sqrt{3}}{8} (1 - 8x) (\mathbf{k} \cdot \mathbf{e}_{3} - \mathbf{k} \cdot \mathbf{e}_{1}) \mathbf{n}_{3}, \\
\vec{\psi}_{4} - \vec{\psi}_{1} = \frac{\sqrt{3}}{4} \frac{D_{x} + D_{z}}{J} (\mathbf{e}_{4} - \mathbf{e}_{1}) + \frac{\sqrt{3}}{8} (1 - 8x) (\mathbf{k} \cdot \mathbf{e}_{4} - \mathbf{k} \cdot \mathbf{e}_{1}) \mathbf{n}_{3},
\end{cases} (27)$$

or, using the additional condition  $\sum_{t=1}^{4} \vec{\psi}_t = 0$ ,

$$\vec{\psi}_t = \frac{\sqrt{3}}{4} \frac{D_x + D_z}{J} \mathbf{e}_t + \frac{\sqrt{3}}{8} (1 - 8x) (\mathbf{k} \cdot \mathbf{e}_t) \mathbf{n}_3, \tag{28}$$

where  $\mathbf{e}_1$ ,  $\mathbf{e}_2$ ,  $\mathbf{e}_3$  and  $\mathbf{e}_4$  are the unit vectors directed along 3-fold symmetry axes corresponding to four sublattices:

$$\begin{cases}
\mathbf{e}_{1} = \frac{1}{\sqrt{3}}(1, 1, 1), \\
\mathbf{e}_{2} = \frac{1}{\sqrt{3}}(-1, 1, -1), \\
\mathbf{e}_{3} = \frac{1}{\sqrt{3}}(-1, -1, 1), \\
\mathbf{e}_{4} = \frac{1}{\sqrt{3}}(1, -1, -1).
\end{cases} (29)$$

Finally, we can express vectors  $\mathbf{n}_{cos}$ ,  $\mathbf{n}_{sin}$  and  $\mathbf{n}_{rot}$  for each of the sublattices:

$$\begin{cases}
\mathbf{n}_{cos}^{t} = \mathbf{n}_{1} + [\vec{\psi}_{t} \times \mathbf{n}_{1}] = \mathbf{n}_{1} + \frac{\sqrt{3}}{4} \frac{D_{x} + D_{z}}{J} [\mathbf{e}_{t} \times \mathbf{n}_{1}] + \frac{\sqrt{3}}{8} (1 - 8x) (\mathbf{k} \cdot \mathbf{e}_{t}) \mathbf{n}_{2}, \\
\mathbf{n}_{sin}^{t} = \mathbf{n}_{2} + [\vec{\psi}_{t} \times \mathbf{n}_{2}] = \mathbf{n}_{2} + \frac{\sqrt{3}}{4} \frac{D_{x} + D_{z}}{J} [\mathbf{e}_{t} \times \mathbf{n}_{2}] - \frac{\sqrt{3}}{8} (1 - 8x) (\mathbf{k} \cdot \mathbf{e}_{t}) \mathbf{n}_{1}, \\
\mathbf{n}_{rot}^{t} = \mathbf{n}_{3} + [\vec{\psi}_{t} \times \mathbf{n}_{3}] = \mathbf{n}_{3} + \frac{\sqrt{3}}{4} \frac{D_{x} + D_{z}}{J} [\mathbf{e}_{t} \times \mathbf{n}_{3}].
\end{cases} (30)$$

Thus, in the common case each sublattice has its own rotation axis different from  $\mathbf{n_k}$  as it shown in Fig. 1(a). The divergence of the axes is defined by Eqs. (30). The substitution of Eqs. (30) into Eq. (5) gives the spin of an individual Mn atom

$$\mathbf{s}_{i} = \left(\mathbf{n}_{1} + \frac{\sqrt{3}}{4} \frac{D_{x} + D_{z}}{J} \left[\mathbf{e}_{t(i)} \times \mathbf{n}_{1}\right] + \frac{\sqrt{3}}{8} (1 - 8x) (\mathbf{k} \cdot \mathbf{e}_{t(i)}) \mathbf{n}_{2}\right) \cos \mathbf{k} \cdot \mathbf{r}_{i} + \left(\mathbf{n}_{2} + \frac{\sqrt{3}}{4} \frac{D_{x} + D_{z}}{J} \left[\mathbf{e}_{t(i)} \times \mathbf{n}_{2}\right] - \frac{\sqrt{3}}{8} (1 - 8x) (\mathbf{k} \cdot \mathbf{e}_{t(i)}) \mathbf{n}_{1}\right) \sin \mathbf{k} \cdot \mathbf{r}_{i},$$

$$(31)$$

The question can arise: why parameter x appears in Eq. (31), in spite of its absence in the initial Eq. (2)? In fact, x is brought in by Eq. (5) depending on real atomic positions. Indeed, parameter x is implicitly involved with atomic coordinates  $\mathbf{r}_i$ , and expressing  $\mathbf{r}$  as

$$\mathbf{r} = \mathbf{p} + \mathbf{r}',\tag{32}$$

with **p** being a period of the crystal or the origin of a unit cell, and  $\mathbf{r}' \in \{(x, x, x), (1 - x, \frac{1}{2} + x, \frac{1}{2} - x), (\frac{1}{2} - x, 1 - x, \frac{1}{2} + x), (\frac{1}{2} + x, \frac{1}{2} - x, 1 - x)\}$  being an atomic position within the cell, and using the condition  $\mathbf{k} \cdot \mathbf{r}' \ll 1$ , we can rewrite Eq. (31) as

$$\mathbf{s}_{i} = \left(\mathbf{n}_{1} + \frac{\sqrt{3}}{4} \frac{D_{x} + D_{z}}{J} \left[\mathbf{e}_{t(i)} \times \mathbf{n}_{1}\right] + \left\{\frac{\sqrt{3}}{8} (1 - 8x)(\mathbf{k} \cdot \mathbf{e}_{t(i)}) + \mathbf{k} \cdot \mathbf{r}'_{t(i)}\right\} \mathbf{n}_{2}\right) \cos \mathbf{k} \cdot \mathbf{p}_{i} + \left(\mathbf{n}_{2} + \frac{\sqrt{3}}{4} \frac{D_{x} + D_{z}}{J} \left[\mathbf{e}_{t(i)} \times \mathbf{n}_{2}\right] - \left\{\frac{\sqrt{3}}{8} (1 - 8x)(\mathbf{k} \cdot \mathbf{e}_{t(i)}) + \mathbf{k} \cdot \mathbf{r}'_{t(i)}\right\} \mathbf{n}_{1}\right) \sin \mathbf{k} \cdot \mathbf{p}_{i},$$

$$(33)$$

where parameter x vanishes in curly brackets after substitution of corresponding e and r'.

Fig. 2 shows spin helix structures calculated with the use of Eq. (31) for directions (001), (111) and (011) of spiral axis in the case of  $\mathbf{n}_3 = \mathbf{n_k}$ . The wave number  $|\mathbf{k}|$  is chosen to be equal to  $2\pi/40$ , which is close to the experimental value for MnSi crystal. The canting **D**-vector component is taken to be rather large,  $D_x + D_z = 0.4J$ , in order to emphasize nonmonotonic frustrated behavior of helices. In this case

$$\frac{|D_x + D_z|}{4J} \gg \frac{(8x - 1)|\mathbf{k}|}{8},\tag{34}$$

and the main contribution in a canting is due to the terms with  $[\mathbf{e}_{t(i)} \times \mathbf{n}_{1,2}]$ .

The extended sinusoids with phase shift of  $\frac{\pi}{2}$  represent spin projections on directions  $\mathbf{n}_1$  and  $\mathbf{n}_2$ , the low ones do spin components along the wave vector, which appear due to the canting. The coloured circles correspond to magnetic atoms in four sublattices of the crystal. Being all different in the common case, the sinusoids connected with different sublattices can coincide for certain directions of  $\mathbf{k}$  reflecting the symmetry. For instance, in the case of  $\mathbf{k} \parallel (001)$  (Fig. 2(a)) the extended sinusoids coincide, which correspond to sublattices 1, 3 and 2, 4; but the circles of different colors do not coincide because the atoms belonging to different sublattices lie in different planes perpendicular to  $\mathbf{k}$ . On the contrary, in the case of  $\mathbf{k} \parallel (111)$  (Fig. 2(b)) coincide both the extended sinusoids and related circles corresponding to sublattices 2, 3, 4, because their sites lie in the same atomic planes perpendicular to  $\mathbf{k}$ . Both two cases, (a) and (b), due to their symmetry ((001) is the axis  $2_1$  and (111) is the axis 3 of the crystal) are characterized by only two extended sinusoids, which defines the view of the black saws representing the angle  $\phi$  between spins in the successive ferromagnetic planes,  $\tan \phi = (\mathbf{s} \cdot \mathbf{n}_2)/(\mathbf{s} \cdot \mathbf{n}_1)$ . The symmetry is also reflected in the low sinusoids corresponding to the spin components parallel to  $\mathbf{k}$ .

When  $\mathbf{k} \parallel (011)$  (Fig. 2(c)) there are three extended sinusoids, which is also reflected in the view of the cooresponding black saw (Fig. 2(d)). In this case, coincide the extended sinusoids corresponding to sublattices 2, 3 and the low ones corresponding to sublattices 1, 4. It may seem from Fig. 2(c) that sublattices 1 and 4 have the same projections on  $\mathbf{k}$ , but it is evident from Fig. 2(d) that it is not so. Indeed, the atoms of types 1 and 4 lie in close but different planes; their proximity is due to the approximate equality  $4x \approx \frac{1}{2}$ .

The "saws" in the figures show a frustration which is the intrinsic feature of the helices due to the spin canting. Owing to the frustration the spins in successive ferromagnetic planes can rotate inversely to twist direction of the helix.

### IV. HELIX IN MAGNETIC FIELD

Let us return to the case of nonzero magnetic field **H**. Numerous experimental data, as well as the results obtained with the use of phenomenological theory, show that in this case the magnetic moments of Mn atoms form a conical helix. The peculiarity of such structure is that the field of magnetic moment possesses a constant component directed along **H**. Then, the spin structure can be described by the following expression

$$\mathbf{s}^{t} = \mathbf{n}_{rot}^{t} \sin \xi + \mathbf{n}_{cos}^{t} \cos \xi \cos \mathbf{k} \cdot \mathbf{r} + \mathbf{n}_{sin}^{t} \cos \xi \sin \mathbf{k} \cdot \mathbf{r}, \tag{35}$$

which satisfies the condition  $|\mathbf{s}^t| = 1$ . Here  $\xi$  is an angle characterizing the ratio between constant and rotating components of the magnetic moments. The substitution of Eq. (35) in the expression (2) and summation over all the

unit cells of the crystal give

$$E_{helix,H} = \frac{N_{cell}}{2} \sum_{i=1}^{4} \sum_{j=1}^{6} (-J \mathbf{n}_{rot}^{i} \cdot \mathbf{n}_{rot}^{t(j)} + \mathbf{D}_{ij} \cdot [\mathbf{n}_{rot}^{i} \times \mathbf{n}_{rot}^{t(j)}]) \sin \xi_{i} \sin \xi_{t}(j)$$

$$+ \frac{N_{cell}}{4} \sum_{i=1}^{4} \sum_{j=1}^{6} \{ (-J \mathbf{n}_{cos}^{i} \cdot \mathbf{n}_{cos}^{t(j)} + \mathbf{D}_{ij} \cdot [\mathbf{n}_{cos}^{i} \times \mathbf{n}_{cos}^{t(j)}]) \cos \mathbf{k} \cdot \mathbf{r}_{ij}$$

$$+ (-J \mathbf{n}_{cos}^{i} \cdot \mathbf{n}_{sin}^{t(j)} + \mathbf{D}_{ij} \cdot [\mathbf{n}_{cos}^{i} \times \mathbf{n}_{sin}^{t(j)}]) \sin \mathbf{k} \cdot \mathbf{r}_{ij}$$

$$- (-J \mathbf{n}_{sin}^{i} \cdot \mathbf{n}_{cos}^{t(j)} + \mathbf{D}_{ij} \cdot [\mathbf{n}_{sin}^{i} \times \mathbf{n}_{cos}^{t(j)}]) \sin \mathbf{k} \cdot \mathbf{r}_{ij}$$

$$+ (-J \mathbf{n}_{sin}^{i} \cdot \mathbf{n}_{sin}^{t(j)} + \mathbf{D}_{ij} \cdot [\mathbf{n}_{sin}^{i} \times \mathbf{n}_{sin}^{t(j)}]) \cos \mathbf{k} \cdot \mathbf{r}_{ij} \} \cos \xi_{i} \cos \xi_{t(j)}$$

$$-N_{cell} g \mu_{B} \sum_{i=1}^{4} \mathbf{H} \cdot \mathbf{n}_{rot}^{i} \sin \xi_{i}.$$

$$(36)$$

Using Eq. (9) we can rewrite the energy up to second order terms on  $|\mathbf{k}| \sim (\omega_i - \omega_{t(j)}) \sim \gamma \sim (D/J)$ :

$$E_{helix,H} = \frac{N_{cell}}{4} \sum_{i=1}^{4} \sum_{j=1}^{6} \{-2J\cos(\xi_{i} - \xi_{t(j)}) + 2\left(\frac{J}{2}(\omega_{i} - \omega_{t(j)} - \mathbf{k} \cdot \mathbf{r}_{ij})^{2} - (\mathbf{D}_{ij} \cdot \mathbf{n}_{3})(\omega_{i} - \omega_{t(j)} - \mathbf{k} \cdot \mathbf{r}_{ij})\right) \cos \xi_{i} \cos \xi_{t(j)} + \left(\frac{J}{2}(\vec{\gamma}_{i} - \vec{\gamma}_{t(j)})^{2} - \mathbf{D}_{ij} \cdot (\vec{\gamma}_{i} - \vec{\gamma}_{t(j)})\right) \left(\cos \xi_{i} \cos \xi_{t(j)} + 2\sin \xi_{i} \sin \xi_{t(j)}\right) + N_{cell}g\mu_{B}(\mathbf{H} \cdot \mathbf{n}_{3}) \sum_{i=1}^{4} \sin \xi_{i}.$$

$$(37)$$

The last term has been obtained supposing that  $g\mu_B H \sim D^2/J$ , which allows us to use approximation  $\mathbf{n}_{rot}^t \approx \mathbf{n}_3$ . The first term in curly brackets has zero order on (D/J) and achieves the minumum, when

$$\xi_1 = \xi_2 = \xi_3 = \xi_4 \equiv \xi. \tag{38}$$

Then, we can rewrite the energy as

$$E_{helix,H} = N_{cell}(-12J + \epsilon_1 \cos^2 \xi + \epsilon_2 (1 + \sin^2 \xi) - 4g\mu_B(\mathbf{H} \cdot \mathbf{n}_3) \sin \xi), \tag{39}$$

where  $\epsilon_1$  and  $\epsilon_2$  are the same as in the previous section. The minimum of the energy (39) is achieved, when  $\mathbf{H} \parallel \mathbf{n}_3$  and  $\mathbf{n}_3 = \mathbf{n}_k$ . Then,

$$E_{helix,H} = N_{cell}J\left(-12 - 2\frac{(D_x + D_z)^2}{J^2} - \frac{1}{3}\frac{(D_x - 2D_y - D_z)^2}{J^2}\cos^2\xi - 4\frac{g\mu_B H}{J}\sin\xi\right),\tag{40}$$

or, after minimization on  $\xi$ ,

$$E_{helix,H} = N_{cell}J\left(-12 - 2\frac{(D_x + D_z)^2}{J^2} - \frac{1}{3}\frac{(D_x - 2D_y - D_z)^2}{J^2} - \frac{12(g\mu_B H)^2}{(D_x - 2D_y - D_z)^2}\right),\tag{41}$$

and

$$\sin \xi = \frac{6Jg\mu_B H}{(D_x - 2D_y - D_z)^2}.$$
(42)

The helix vanishes, when  $\xi = \frac{\pi}{2}$ , which corresponds to magnetic field

$$H_c = \frac{(D_x - 2D_y - D_z)^2}{6Jg\mu_B}. (43)$$

(this field, unwinding the helix, is usually called  $H_{c2}$  [22]).

Thus, in the approximation used here, the wave vector  $\mathbf{k}$  is directed along the applied magnetic field. The spin structure for each sublattice obtains a permanent component along its rotation axis  $\mathbf{n}_{rot}$ , which is different from direction  $\mathbf{n}_{\mathbf{k}} \parallel \mathbf{H}$ , see Fig. 1(b). The helices become conical, and as the magnetic field increases up to  $H_c$ , the permanent components grow proportionally to the field value, Eq. (42), whereas the rotated components decrease correspondingly. It should be noted that if the field is less than  $H_c$ , it does not affect the axes  $\mathbf{n}_{rot}$  and they have the same directions, defined by Eq. (28), as in the absence of magnetic field.

#### V. COARSE GRAIN APPROXIMATION

In the phenomenological theory, the energy of chiral magnetics is usually written as

$$E = \int \left( \mathcal{J} \frac{\partial M_n}{\partial r_m} \frac{\partial M_n}{\partial r_m} + \mathcal{D} \mathbf{M} \cdot [\vec{\nabla} \times \mathbf{M}] \right) d\mathbf{r}, \tag{44}$$

where  $\mathbf{M}(\mathbf{r})$  is the local magnetic moment changing smoothly in space. Below it will be shown how this equation and phenomenological coefficients  $\mathcal{J}$  and  $\mathcal{D}$  arise from microscopic consideration based on Eq. (2).

Let us suppose that the typical scale at which a considerable change of magnetic moment occurs is much bigger than the size of the unit cell, and any two neighboring spins are rotated relative to each another by a small angle of order (D/J). Let  $\mathbf{s}_i$  and  $\mathbf{s}_j$  be the neighboring spins and  $\mathbf{s}_j = R(\vec{\zeta}_{ij})\mathbf{s}_i$ , or

$$\mathbf{s}_{j} = \mathbf{s}_{i} \cos \zeta_{ij} + \frac{\sin \zeta_{ij}}{\zeta_{ij}} [\vec{\zeta}_{ij} \times \mathbf{s}_{i}] + \frac{1 - \cos \zeta_{ij}}{\zeta_{ij}^{2}} \vec{\zeta}_{ij} (\vec{\zeta}_{ij} \cdot \mathbf{s}_{i}), \tag{45}$$

where  $\zeta_{ij} \equiv |\vec{\zeta}_{ij}|$ . Then,

$$\mathbf{s}_{i} \cdot \mathbf{s}_{j} \approx 1 - \zeta_{ij}^{2}/2 + (\mathbf{s}_{i} \cdot \vec{\zeta}_{ij})^{2}/2 = 1 - \zeta_{ij}^{2}/2,$$
 (46)

$$[\mathbf{s}_i \times \mathbf{s}_j] \approx \vec{\zeta}_{ij} - \mathbf{s}_i(\mathbf{s}_i \cdot \vec{\zeta}_{ij}) = \vec{\zeta}_{ij\perp},$$
 (47)

where  $\vec{\zeta}_{ij\perp}$  is the part of vector  $\vec{\zeta}_{ij}$  perpendicular to unit vector  $\mathbf{s}_i$ .

If spins vary slowly along the crystal, we can take a domain, which is much bigger than a unit cell, but small enough as compared with the scale at wich a considerable change of spin occures. The spins within this domain are almost unidirectional. Consequently, all the vectors  $\vec{\zeta}_{ij\perp}$  nearly lie in a plane. Let us neglect this "nearly" and suppose that all  $\vec{\zeta}_{ij\perp}$  belong to the plane perpendicular to some mean spin s. In addition, staying in the domain, we can discard the parts of  $\vec{\zeta}_{ij}$  parallel to s and suppose that  $\vec{\zeta}_{ij\perp} = \vec{\zeta}_{ij}$ .

Another simplification can be achieved with taking into account that a spin does not change upon round a close chain of atoms. This means that the sum of small angles  $\vec{\zeta}_{ij}$  corresponding to the bonds of the chain should be equal to zero. For instance, for the triangle formed by spins  $\mathbf{s}_1$ ,  $\mathbf{s}_2$  and  $\mathbf{s}_3$  we obtain the following condition

$$\vec{\zeta}_{12} + \vec{\zeta}_{23} + \vec{\zeta}_{31} = 0, \tag{48}$$

which is evidently satisfied, if  $\vec{\zeta}_{ij} = \vec{\zeta}_j - \vec{\zeta}_i$ , where  $\vec{\zeta}_i$  and  $\vec{\zeta}_j$  are perpendicular to **s** vectors associated with *i*-th and *i*-th atoms.

With the approximations accepted, using the expressions (46) and (47), the energy (2) in the absence of magnetic field can be now rewritten as

$$E = \frac{1}{2} \sum_{i} \sum_{j=1}^{6} \left( -J + \frac{J}{2} (\vec{\zeta}_{j} - \vec{\zeta}_{i})^{2} + \mathbf{D}_{ij} \cdot (\vec{\zeta}_{j} - \vec{\zeta}_{i}) \right). \tag{49}$$

The minimization of the energy on the vector  $\vec{\zeta}_i$  associated with *i*-th atom and belonging to the plane perpendicular to **s** gives

$$\frac{\partial E}{\partial \vec{\zeta_i}} = -\sum_{j=1}^{6} (J(\vec{\zeta_j} - \vec{\zeta_i}) + \mathbf{D}_{ij\perp}) = 0, \tag{50}$$

or

$$\vec{\zeta}_{i} = \frac{1}{6} \sum_{j=1}^{6} \vec{\zeta}_{j} + \frac{1}{6J} \left( \sum_{j=1}^{6} \mathbf{D}_{ij} \right) = \frac{1}{6} \sum_{j=1}^{6} \vec{\zeta}_{j} + \frac{1}{\sqrt{3}} \frac{D_{x} + D_{z}}{J} \mathbf{e}_{t(i)\perp},$$
 (51)

where symbol " $\perp$ " designates the projection of a vector to the plane perpendicular to  $\mathbf{s}$ ,  $\mathbf{e}_{t(i)}$  is one of the vectors (29). The last therm in the right part of (51) reflects the evident fact that the sum of DM vectors associated with all the bonds of an atom should be parallel to the 3-fold axis to which the atomic position belongs.

Let us introduce a new vector  $\tilde{\vec{\zeta}}_i$  connected with the old one by equation

$$\vec{\zeta}_i = \tilde{\vec{\zeta}}_i + A\mathbf{e}_{t(i)\perp}. \tag{52}$$

where A is a constant. Then,

$$\tilde{\zeta}_{i} = \frac{1}{6} \sum_{j=1}^{6} \tilde{\zeta}_{j} + \left( -\frac{4}{3} A + \frac{1}{\sqrt{3}} \frac{D_{x} + D_{z}}{J} \right) \mathbf{e}_{t(i)\perp}, \tag{53}$$

where it has been taken into account that an atom belonging to one of four sublattices has two neighbors at each of three remaining ones, so

$$\sum_{j=1}^{6} \mathbf{e}_{t(j)} = -2\mathbf{e}_{t(i)}.$$
(54)

Choosing

$$A = \frac{\sqrt{3}}{4} \frac{D_x + D_z}{J},\tag{55}$$

we can now write

$$\vec{\zeta}_i = \tilde{\zeta}_i^{\vec{i}} + \frac{\sqrt{3}}{4} \frac{D_x + D_z}{J} \mathbf{e}_{t(i)\perp}, \tag{56}$$

$$\tilde{\vec{\zeta}}_i = \frac{1}{6} \sum_{j=1}^6 \tilde{\vec{\zeta}}_j, \tag{57}$$

and, after the substitution of Eq. (56) into Eq. (49),

$$E = \frac{1}{2} \sum_{i} \sum_{j=1}^{6} \left\{ -J + \frac{J}{2} (\tilde{\zeta}_{j} - \tilde{\zeta}_{i})^{2} + \tilde{\mathbf{D}}_{ij} \cdot (\tilde{\zeta}_{j} - \tilde{\zeta}_{i}) \right\} + \frac{1}{2} \sum_{i} \sum_{j=1}^{6} \left\{ \frac{3}{32} \frac{(D_{x} + D_{z})^{2}}{J} (\mathbf{e}_{t(j)} - \mathbf{e}_{t(i)})_{\perp}^{2} + \frac{\sqrt{3}}{4} \frac{D_{x} + D_{z}}{J} \mathbf{D}_{ij} \cdot (\mathbf{e}_{t(j)} - \mathbf{e}_{t(i)})_{\perp} \right\},$$

$$(58)$$

where

$$\tilde{\mathbf{D}}_{ij} = \mathbf{D}_{ij} + \frac{\sqrt{3}}{4} (D_x + D_z) (\mathbf{e}_{t(j)} - \mathbf{e}_{t(i)}) 
= \mathbf{D}_{ij} + \frac{1}{8} \left( \sum_{j'=1}^{6} \mathbf{D}_{t(j)j'} - \sum_{j''=1}^{6} \mathbf{D}_{t(i)j''} \right).$$
(59)

The first part of Eq. (58) is analogous to the expression (49), but with modificated DM vectors. It is important here that the combination  $(\mathbf{e}_{t(j)} - \mathbf{e}_{t(i)})$  varies from bond to bond with the use of the same symmetry transformations of the point group  $m\bar{3}$  as vector  $\mathbf{D}_{ij}$  and, consequently,  $\tilde{\mathbf{D}}_{ij}$ . The vectors  $\tilde{\mathbf{D}}_{ij}$  are characterized by condition  $\tilde{D}_x + \tilde{D}_z = 0$ , so they have only two independent components. For example, the modificated DM vector of the bond  $(-2x, \frac{1}{2}, \frac{1}{2} - 2x)$  is

$$\tilde{\mathbf{D}} = (D_x, D_y, D_z) + \frac{\sqrt{3}}{4}(D_x + D_z)(\mathbf{e}_2 - \mathbf{e}_1) = \left(\frac{D_x - D_z}{2}, D_y, -\frac{D_x - D_z}{2}\right).$$
(60)

The second part of Eq. (58) contains the terms like

$$\mathbf{a}_{\perp} \cdot \mathbf{b}_{\perp} = \mathbf{a} \cdot \mathbf{b} - (\mathbf{a} \cdot \mathbf{s})(\mathbf{b} \cdot \mathbf{s}),\tag{61}$$

depending on the direction of **s**. The vectors **a** and **b** vary from bond to bond with the use of the symmetry transformations of the point group 23, and the averaging over 12 bonds in the unit cell, as well as for the case of the averaging over the sphere, gives

$$\langle \mathbf{a}_{\perp} \cdot \mathbf{b}_{\perp} \rangle = \mathbf{a} \cdot \mathbf{b} - \frac{1}{12} \sum_{n=1}^{12} ((R_n \mathbf{a}) \cdot \mathbf{s})((R_n \mathbf{b}) \cdot \mathbf{s}) = \mathbf{a} \cdot \mathbf{b} - \frac{1}{3} \mathbf{a} \cdot \mathbf{b} = \frac{2}{3} \mathbf{a} \cdot \mathbf{b}, \tag{62}$$

with  $R_n$  being the rotation matrices of the group 23. Thereby, the mean contribution of the second part of Eq. (58) to the energy of a bond is

$$\frac{2}{3} \left\{ \frac{3}{32} \frac{(D_x + D_z)^2}{J} (\mathbf{e}_2 - \mathbf{e}_1)^2 + \frac{\sqrt{3}}{4} \frac{D_x + D_z}{J} (D_x, D_y, D_z) \cdot (\mathbf{e}_2 - \mathbf{e}_1) \right\} = -\frac{(D_x + D_z)^2}{6J},\tag{63}$$

and we can now rewrite the expression (58) for the energy as

$$E = \frac{1}{2} \sum_{i} \sum_{j=1}^{6} \left\{ \frac{J}{2} (\tilde{\zeta}_{j}^{j} - \tilde{\zeta}_{i}^{j})^{2} + \tilde{\mathbf{D}}_{ij} \cdot (\tilde{\zeta}_{j}^{j} - \tilde{\zeta}_{i}^{j}) \right\} + N_{cell} J \left( -12 - 2 \left( \frac{D_{x} + D_{z}}{J} \right)^{2} \right).$$
 (64)

Let us introduce now smooth continuous vector fields  $\hat{\vec{\zeta}}_1(\mathbf{r})$ ,  $\hat{\vec{\zeta}}_2(\mathbf{r})$ ,  $\hat{\vec{\zeta}}_3(\mathbf{r})$  and  $\hat{\vec{\zeta}}_4(\mathbf{r})$ , connecting with  $\tilde{\vec{\zeta}}_i$  by the equation

$$\tilde{\vec{\zeta}}_i = \hat{\vec{\zeta}}_{t(i)}(\mathbf{r}_i). \tag{65}$$

We can suppose that functions  $\hat{\vec{\zeta}_t}$  change slowly enough with coordinates and postulate the homogeneity condition

$$\frac{\partial(\hat{\vec{\zeta}}_1)_n}{\partial r_m} = \frac{\partial(\hat{\vec{\zeta}}_2)_n}{\partial r_m} = \frac{\partial(\hat{\vec{\zeta}}_3)_n}{\partial r_m} = \frac{\partial(\hat{\vec{\zeta}}_4)_n}{\partial r_m} \equiv \frac{\partial\hat{\zeta}_n}{\partial r_m}, \quad m, n = 1, 2, 3,$$
(66)

reflecting the fact that the divergence between sublattices is preserved over big distances. Then, we can write Eq. (57) for 1st atom in a cell in the explicit form as

$$\hat{\zeta}_{1}(x,x,x) = \frac{1}{6} \left( \hat{\zeta}_{2}(-x, \frac{1}{2} + x, \frac{1}{2} - x) + \hat{\zeta}_{2}(-x, -\frac{1}{2} + x, \frac{1}{2} - x) + \hat{\zeta}_{3}(\frac{1}{2} - x, -x, \frac{1}{2} + x) + \hat{\zeta}_{3}(\frac{1}{2} - x, -x, -\frac{1}{2} + x) + \hat{\zeta}_{4}(\frac{1}{2} + x, \frac{1}{2} - x, -x) + \hat{\zeta}_{4}(-\frac{1}{2} + x, \frac{1}{2} - x, -x) \right) 
= \frac{1}{3} \left( \hat{\zeta}_{2}(x, x, x) + \hat{\zeta}_{3}(x, x, x) + \hat{\zeta}_{4}(x, x, x) + \frac{1}{6} \left( \sum_{j=1}^{6} \mathbf{r}_{1j} \cdot \vec{\nabla} \right) \hat{\zeta}(x, x, x) \right).$$
(67)

The last equation is correct not only for  $\mathbf{r} = (x, x, x)$  but also for arbitrary  $\mathbf{r}$  due to homogeneity condition. So, we can write Eq. (67) and analogous equations for other atoms in a cell, supposing that all  $\hat{\zeta}_i$  are taken at the same point:

$$\begin{cases}
\hat{\zeta}_{1}^{i} = \frac{1}{3} \left( \hat{\zeta}_{2}^{i} + \hat{\zeta}_{3}^{i} + \hat{\zeta}_{4}^{i} \right) + \frac{1}{6} \left( \sum_{j=1}^{6} \mathbf{r}_{1j} \cdot \vec{\nabla} \right) \hat{\zeta}^{i}, \\
\hat{\zeta}_{2}^{i} = \frac{1}{3} \left( \hat{\zeta}_{1}^{i} + \hat{\zeta}_{3}^{i} + \hat{\zeta}_{4}^{i} \right) + \frac{1}{6} \left( \sum_{j=1}^{6} \mathbf{r}_{2j} \cdot \vec{\nabla} \right) \hat{\zeta}^{i}, \\
\hat{\zeta}_{3}^{i} = \frac{1}{3} \left( \hat{\zeta}_{1}^{i} + \hat{\zeta}_{2}^{i} + \hat{\zeta}_{4}^{i} \right) + \frac{1}{6} \left( \sum_{j=1}^{6} \mathbf{r}_{3j} \cdot \vec{\nabla} \right) \hat{\zeta}^{i}, \\
\hat{\zeta}_{4}^{i} = \frac{1}{3} \left( \hat{\zeta}_{1}^{i} + \hat{\zeta}_{2}^{i} + \hat{\zeta}_{3}^{i} \right) + \frac{1}{6} \left( \sum_{j=1}^{6} \mathbf{r}_{4j} \cdot \vec{\nabla} \right) \hat{\zeta}^{i}.
\end{cases} (68)$$

The system (68) is degenerate on variables  $\hat{\vec{\zeta}}_1$ ,  $\hat{\vec{\zeta}}_2$ ,  $\hat{\vec{\zeta}}_3$ ,  $\hat{\vec{\zeta}}_4$  and satisfied, when

$$\hat{\vec{\zeta}}_t - \hat{\vec{\zeta}}_{t'} = \frac{1}{8} \left( \sum_{j=1}^6 \mathbf{r}_{tj} \cdot \vec{\nabla} - \sum_{j'=1}^6 \mathbf{r}_{t'j'} \cdot \vec{\nabla} \right) \hat{\vec{\zeta}}. \tag{69}$$

Let us allocate two parts from expression (64) for the energy associated with a unit cell,

$$E_{cell,exch} = \frac{J}{4} \sum_{i=1}^{4} \sum_{j=1}^{6} (\hat{\vec{\zeta}}_{t(j)}(\mathbf{r}_j) - \hat{\vec{\zeta}}_{i}(\mathbf{r}_i))^2 = \frac{J}{4} \sum_{i=1}^{4} \sum_{j=1}^{6} (\hat{\vec{\zeta}}_{t(j)} - \hat{\vec{\zeta}}_{i} + (\mathbf{r}_{ij} \cdot \vec{\nabla})\hat{\vec{\zeta}})^2$$
 (70)

and

$$E_{cell,DM} = \frac{1}{2} \sum_{i=1}^{4} \sum_{j=1}^{6} \tilde{\mathbf{D}}_{ij} \cdot (\hat{\vec{\zeta}}_{t(j)}(\mathbf{r}_{j}) - \hat{\vec{\zeta}}_{i}(\mathbf{r}_{i})) = \frac{1}{2} \sum_{i=1}^{4} \sum_{j=1}^{6} \tilde{\mathbf{D}}_{ij} \cdot (\hat{\vec{\zeta}}_{t(j)} - \hat{\vec{\zeta}}_{i} + (\mathbf{r}_{ij} \cdot \vec{\nabla})\hat{\vec{\zeta}}).$$
(71)

With the use of Eq. (69) we can rewrite these parts as

$$E_{cell,exch} = -\frac{J}{16} \sum_{i=1}^{4} \left( \left( \sum_{j=1}^{6} \mathbf{r}_{ij} \cdot \vec{\nabla} \right) \hat{\zeta} \right)^{2} + \frac{J}{4} \sum_{i=1}^{4} \sum_{j=1}^{6} \left( (\mathbf{r}_{ij} \cdot \vec{\nabla}) \hat{\zeta} \right)^{2}$$
(72)

and

$$E_{cell,DM} = \frac{1}{2} \sum_{i=1}^{4} \sum_{j=1}^{6} (\mathbf{r}_{ij} \cdot \vec{\nabla}) (\tilde{\mathbf{D}}_{ij} \cdot \hat{\vec{\zeta}}) - \frac{1}{8} \sum_{i=1}^{4} \left( \sum_{j=1}^{6} \mathbf{r}_{ij} \cdot \vec{\nabla} \right) \left( \sum_{j'=1}^{6} \tilde{\mathbf{D}}_{ij'} \cdot \hat{\vec{\zeta}} \right).$$
(73)

The second part of (73) vanishes, because

$$\sum_{i=1}^{6} \tilde{\mathbf{D}}_{ij} = 0. \tag{74}$$

Using

$$\sum_{j=1}^{6} \mathbf{r}_{ij} = \sqrt{3}(1 - 8x)\mathbf{e}_i,\tag{75}$$

the first part of (72) can be calculated,

$$-\frac{J}{16} \sum_{i=1}^{4} \left( \left( \sum_{j=1}^{6} \mathbf{r}_{ij} \cdot \vec{\nabla} \right) \hat{\vec{\zeta}} \right)^{2} = -\frac{J}{4} (1 - 8x)^{2} \frac{\partial \hat{\zeta}_{n}}{\partial r_{m}} \frac{\partial \hat{\zeta}_{n}}{\partial r_{m}}.$$
 (76)

The second part of (72) can be expressed as

$$\frac{J}{4} \sum_{\alpha=1}^{24} R_{kl}^{\alpha} R_{mn}^{\alpha} ((\mathbf{r}_{12})_l \nabla_k \hat{\zeta}) \cdot ((\mathbf{r}_{12})_n \nabla_m \hat{\zeta}) = J(1 - 4x + 16x^2) \frac{\partial \hat{\zeta}_n}{\partial r_m} \frac{\partial \hat{\zeta}_n}{\partial r_m}, \tag{77}$$

where summation is taken over all elements  $R^{\alpha}$  of the point symmetry group  $m\bar{3}$ , and we have used that

$$\sum_{\alpha=1}^{24} R_{kl}^{\alpha} R_{mn}^{\alpha} = 8\delta_{km} \delta_{ln} \tag{78}$$

and

$$(\mathbf{r}_{12})^2 = \frac{1}{2}(1 - 4x + 16x^2). \tag{79}$$

So, finally,

$$E_{cell,exch} = \frac{3J}{4} \frac{\partial \hat{\zeta}_n}{\partial r_m} \frac{\partial \hat{\zeta}_n}{\partial r_m}.$$
 (80)

Similarly, Eq. (73) can be rewritten as

$$E_{cell,DM} = \sum_{\alpha=1}^{24} R_{kl}^{\alpha} R_{mn}^{\alpha}(\mathbf{r}_{12})_l(\tilde{\mathbf{D}}_{12})_n \nabla_k \hat{\zeta}_m = 4(\mathbf{r}_{12} \cdot \tilde{\mathbf{D}}_{12}) \frac{\partial \hat{\zeta}_n}{\partial r_n}$$
(81)

or

$$E_{cell,DM} = -(D_x - 2D_y - D_z) \frac{\partial \hat{\zeta}_n}{\partial r_n}.$$
 (82)

It should be noted that, whereas Eqs. (72) and (73) contain parameter x, the resulting expressions (80) and (82) do not depend on x. This looks like a coincidence, but it is not so. Indeed, the initial statement of the problem do not include atomic coordinates (e.g., see Eq. (1)), and therefore the coordinates will not appear in results (at least until strong changes of the coordinates changing the topology of the net of nearest neighbors).

The substitution of Eqs. (80) and (82) into Eq. (64) gives

$$E = \int \left( \mathcal{J} \frac{\partial \hat{\zeta}_n}{\partial r_m} \frac{\partial \hat{\zeta}_n}{\partial r_m} - \mathcal{D} \frac{\partial \hat{\zeta}_n}{\partial r_n} \right) d\mathbf{r} + N_{cell} J \left( -12 - 2 \left( \frac{D_x + D_z}{J} \right)^2 \right), \tag{83}$$

with  $\mathcal{J}$  and  $\mathcal{D}$  given by the following equations

$$\mathcal{J} = \frac{3J}{4},\tag{84}$$

$$\mathcal{D} = -4(\mathbf{r}_{12} \cdot \tilde{\mathbf{D}}_{12}) = D_x - 2D_y - D_z. \tag{85}$$

The summation over all unit cells of the crystal has been replaced with the integration over the crystal volume. Let us suppose that the vector field  $\hat{\vec{\zeta}}$  is connected with a spin field  $\hat{\mathbf{s}}$ :

$$\hat{\mathbf{s}} \approx \mathbf{s}_0 + [\hat{\vec{\zeta}} \times \mathbf{s}_0], \tag{86}$$

where  $\mathbf{s}_0$  is a constant vector,  $\hat{\vec{\zeta}} \perp \mathbf{s}_0$ . Then,

$$\frac{\partial \hat{s}_n}{\partial r_m} \frac{\partial \hat{s}_n}{\partial r_m} \approx \frac{\partial \hat{\zeta}_n}{\partial r_m} \frac{\partial \hat{\zeta}_n}{\partial r_m} \tag{87}$$

and

$$\hat{\mathbf{s}} \cdot [\vec{\nabla} \times \hat{\mathbf{s}}] \approx -\frac{\partial \hat{\zeta}_n}{\partial x_n}.$$
 (88)

So, we can rewrite Eq. (83) for the energy as

$$E = \int \left( \mathcal{J} \frac{\partial \hat{\mathbf{s}}_n}{\partial r_m} \frac{\partial \hat{\mathbf{s}}_n}{\partial r_m} + \mathcal{D} \hat{\mathbf{s}} \cdot [\vec{\nabla} \times \hat{\mathbf{s}}] \right) d\mathbf{r} + N_{cell} J \left( -12 - 2 \left( \frac{D_x + D_z}{J} \right)^2 \right), \tag{89}$$

the first part of which coincides with the usually used energy in the phenomenological theory with the elastic constants  $\mathcal{J}$  and  $\mathcal{D}$  related to the the constants of microscopic interactions by Eqs. (84) and (85).

The wave number for the helix structure can be now found using the phenomenological approach,

$$k = \frac{\mathcal{D}}{2\mathcal{J}} = \frac{2}{3} \left( \frac{D_x - 2D_y - D_z}{J} \right),\tag{90}$$

which coincides with Eq. (25).

Thus, we have passed from the discrete spin distribution of the microscopic theory to the continuous spin field  $\hat{\mathbf{s}}$  of the coarse grain theory. In order to complete our reasoning we can also consider the way back from the continuous approximation to dicrete spin distribution.

Let  $\hat{\mathbf{s}}(\mathbf{r})$  be a continuous spin field from the phenomenological theory. Within a small domain of the crystal we can associate with  $\hat{\mathbf{s}}$  a vector field  $\hat{\vec{\zeta}}$  using the transformation inverse to (86):

$$\hat{\vec{\zeta}} = [\mathbf{s}_0 \times \hat{\mathbf{s}}]. \tag{91}$$

Here  $\mathbf{s}_0$  is some mean value of  $\hat{\mathbf{s}}$ , which is constant over the domain. Then,

$$\frac{\partial \hat{\vec{\zeta}}}{\partial r_n} = [\mathbf{s}_0 \times \frac{\partial \hat{\mathbf{s}}}{\partial r_n}] \approx [\hat{\mathbf{s}} \times \frac{\partial \hat{\mathbf{s}}}{\partial r_n}]. \tag{92}$$

Let us define continuous fields  $\hat{\vec{\zeta}}_1$ ,  $\hat{\vec{\zeta}}_2$ ,  $\hat{\vec{\zeta}}_3$  and  $\hat{\vec{\zeta}}_4$  for four sublattices of magnetic atoms by formula

$$\hat{\vec{\zeta}}_t = \hat{\vec{\zeta}} + \frac{1}{8} \sum_{j=1}^{6} (\mathbf{r}_{tj} \cdot \vec{\nabla}) \hat{\vec{\zeta}}, \tag{93}$$

obviously obeying Eq. (69). Thus  $\hat{\vec{\zeta}}$  is the average of these four fields,

$$\hat{\vec{\zeta}} = \frac{1}{4}(\hat{\vec{\zeta}}_1 + \hat{\vec{\zeta}}_2 + \hat{\vec{\zeta}}_3 + \hat{\vec{\zeta}}_4). \tag{94}$$

Then, using Eqs. (65) and (56) we can express vector  $\vec{\zeta}_i$  for individual atom trough  $\hat{\vec{\zeta}}$ ,

$$\vec{\zeta}_{i} = \hat{\vec{\zeta}}(\mathbf{r}_{i}) + \frac{\sqrt{3}}{4} \frac{D_{x} + D_{z}}{J} \mathbf{e}_{t(i)\perp}(\mathbf{r}_{i}) + \frac{\sqrt{3}}{8} (1 - 8x)(\mathbf{e}_{t(i)} \cdot \vec{\nabla}) \hat{\vec{\zeta}}(\mathbf{r}_{i}), \tag{95}$$

where

$$\mathbf{e}_{t(i)\perp}(\mathbf{r}_i) = \mathbf{e}_{t(i)} - \hat{\mathbf{s}}(\mathbf{r}_i)(\hat{\mathbf{s}}(\mathbf{r}_i) \cdot \mathbf{e}_{t(i)}). \tag{96}$$

The substitution of Eq. (95) into the equation

$$\mathbf{s}_i = \hat{\mathbf{s}} + [\vec{\zeta}_i \times \hat{\mathbf{s}}] \tag{97}$$

gives us the following expression for the spin of individual magnetic atom

$$\mathbf{s}_{i} = \hat{\mathbf{s}}(\mathbf{r}_{i}) + \frac{\sqrt{3}}{4} \frac{D_{x} + D_{z}}{J} [\mathbf{e}_{t(i)} \times \hat{\mathbf{s}}(\mathbf{r}_{i})] + \frac{\sqrt{3}}{8} (1 - 8x) (\mathbf{e}_{t(i)} \cdot \vec{\nabla}) \hat{\mathbf{s}}(\mathbf{r}_{i}). \tag{98}$$

This equation is valid for any smooth continuous field  $\hat{\mathbf{s}}(\mathbf{r})$ . For one-dimensional helices, the first term in Eq. (98), which is common for all sublattices, describes spin rotation in the plane perpendicular to the wave vector  $\mathbf{k}$ , the second one defines a spin component parallel to  $\mathbf{k}$ , and second and third ones taken together do a shift of the phase of the rotation for each sublattice. For instance, if one chooses  $\hat{\mathbf{s}}$  in the form of

$$\hat{\mathbf{s}}(\mathbf{r}) = \mathbf{n}_1 \cos \mathbf{k} \cdot \mathbf{r} + \mathbf{n}_2 \sin \mathbf{k} \cdot \mathbf{r},\tag{99}$$

then  $\mathbf{s}_i = \mathbf{s}^{t(i)}(\mathbf{r}_i)$  has the form (31).

#### VI. DISCUSSION AND SUMMARY

As it is shown above, in the approximation linear on (D/J), only two components of DM vectors are significant for the considered magnetic structure of MnSi:  $D_x - 2D_y - D_z$  and  $D_x + D_z$ . The third component,  $D_x + D_y - D_z$ , appears in upper approximations. The pseudo-scalar constant  $\mathcal{D}$  used in the phenomenological theory is found to be proportional to the first component,  $D_x - 2D_y - D_z$ . In fact, we could expect that only this combination of **D**-vector coordinates played a role in the simplest microscopic approximation. Surprisingly, it has been found that another component,  $D_x + D_z$ , is also very important both because of its contribution into magnetic energy and its influence on spins orientations. This effect is very similar to "frozen" optical phonon displacements of atoms in crystals. Whereas the former component is responsible for the long scale chiral magnetic structure, the latter leads to a canting of spins within a unit cell and this canting could be in principle measured experimentally using diffraction methods [23]. For instance, for the magnetic fields stronger than  $H_c$ , the residual splay of spins results in non-zero value of the neutron scattering amplitude for reflections of  $00\ell$ ,  $\ell = 2n+1$  type, forbidden both for nuclear scattering and for ferromagnetic scattering owing to  $2_1$  screw axes.

An interesting result about the symmetry of the problem can be revealed considering the inverse structure, where magnetic atoms occupy positions (-x, -x, -x) rather than (x, x, x). The crystal thus obtained has the same space group,  $P2_13$ , but both the crystals are related as right- and left-hand structures, via the inversion transformation. It can be easily seen from the expression (1) that energy does not change over this transformation, if the spins in corresponding positions are equal and so do Dzyaloshinskii-Moriya vectors associated with corresponding bonds. This means that DM vectors are really pseudovectors. Also it is well understood [14, 15] that the inversion should change the chirality of the structure and, consequently, the sign of phenomenological constant  $\mathcal{D}$  and wave number k. However it is not so evident from Eq. (90) that k changes its sign over inversion, because  $\mathbf{D}$  is a pseudovector rather than a vector. We should rewrite the wave number in an invariant form, including an explicit dependence on the bond direction, in order to make transparent the change of chirality upon inversion:

$$k = -\frac{8(\mathbf{r}_{12} \cdot \tilde{\mathbf{D}}_{12})}{3J}.\tag{100}$$

The pseudovector  $\tilde{\mathbf{D}}_{12}$  does not change its sign under inversion but  $\mathbf{r}_{12}$  does. Notice that in this form the sign of k does not depend on our choice which of atoms is 1 or 2.

It is interesting to compare our results with those ones obtained by Hopkinson and Kee [18] using mean-field and real-space rigid rotor minimization methods. According to this work, for both methods, a sizable spin helicity can be obtained only when the DM vectors lie parallel to the corresponding Mn-Mn bonds. Correspondingly, three components of DM vector are considered: the first one, parallel to the bond, the second one, perpendicular to the triangle of bonds, to which this bond is belonging, and the third one, lying in the plane of the triangle, but perpendicular to the bond. For instance, for the bond  $\mathbf{r}_{12} = (-2x, \frac{1}{2}, \frac{1}{2} - 2x)$  these three directions can be written in explicit form as  $(-2x, \frac{1}{2}, \frac{1}{2} - 2x)$ , (1, 1, -1) and  $(1 - 2x, 4x - \frac{1}{2}, \frac{1}{2} + 2x)$ , correspondingly, or, using x = 0.138, as (-0.276, 0.5, 0.224), (1, 1, -1) and (0.724, 0.052, 0.776). The first component is responsible for the helix structure, and corresponding direction, (-0.276, 0.5, 0.224), is very close to direction (-1, 2, 1) for  $D_x - 2D_y - D_z$  component found in our work (the angle between them is about 3.4 degrees). The second component, which does not cant spins [18], coincides with our "neutral" component  $D_x + D_y - D_z$  directed along the corresponding 3-fold axis. The third

component leads to spin canting and rather small spin spiraling, and its direction, (0.724, 0.052, 0.776), is very close to direction (1,0,1) for  $D_x + D_z$  component. Obviously, those numerical results almost coincide with our analytical solutions. An advantage of the analytical solution is that it does not rely on the exact bond directions and atomic coordinates; that is natural from the theoretical point of view because the atomic parameter x does not figure in Eq. 1.

Moreover, different model considerations predict that the superexchange DM vectors are either perpendicular [24] or almost perpendicular [25–27] to the corresponding bonds. If this is also the case in MnSi, we could expect pronounced frustration of the helices. In any case, it is obvious that modern *ab initio* calculations of the Dyzaloshinskii-Moriya vectors would be very important for MnSi-type crystals.

In conclusion, it is found which component of the Dyzaloshinskii-Moriya vector determines the long-range spiral ordering. The most interesting point is that the local structure of helices can be rather complicated owing to symmetry-driven frustrations. We hope that qualitatively all the considered features will appear also in more sophisticated models taking into account the itinerant nature of magnetism and thermal and quantum properties of spiral ordering in MnSi.

#### Acknowledgements

We are grateful to S. V. Grigoriev and S. V. Maleyev for useful discussions. This work was supported by two basic research programs of the Presidium of the Russian Academy of Sciences: "Thermophysics and Mechanics of Extreme Energy Actions and the Physics of a Strongly Compressed Substance" and "Resonant X-ray Diffraction and Topography in Forbidden Reflections".

- [1] A. A. Kornyshev, D. J. Lee, S. Leikin, and A. Wynveen, Rev. Mod. Phys., 79, 943 (2007).
- [2] V. A. Belyakov and V. E. Dmitrienko, Sov. Phys. Usp., 28, 535 (1985); Usp. Fiz. Nauk, 146, 369 (1985).
- [3] D. C. Wright and N. D. Mermin, Rev. Mod. Phys. 61, 385, (1989).
- [4] A. N. Bogdanov and D. A. Yablonskii, Sov. Phys. JETP 68, 101 (1989).
- [5] U. K. Rößler, A. N. Bogdanov, and C. Pfleiderer, Nature 442 797 (2006).
- [6] X. Z. Yu, N. Kanazawa, Y. Onose, K. Kimoto, W. Z. Zhang, S. Ishiwata, Y. Matsui, and Y. Tokura, Nature Mat. 10, 106 (2011).
- [7] S. Tewari, D. Belitz, and T. R. Kirkpatrick, Phys. Rev. Lett. 96, 047207 (2006).
- [8] O. Nakanishi, A. Yanase, A. Hasegawa, and M. Kataoka, Solid State Commun. 35, 995 (1980).
- [9] P. Bak and M. H. Jensen, J. Phys. C: Solid State Phys. 13, L881 (1980).
- [10] I. E. Dzyaloshinsky, Zh. Eksp. Teor. Fiz. 32, 1547 (1957); Sov. Phys. JETP, 5, 1259 (1957).
- [11] I. Dzyaloshinsky, J. Phys. Chem. Solids 4, 241 (1958).
- [12] T. Moriya, Phys. Rev. Lett. 4, 228 (1960).
- [13] T. Moriya, Phys. Rev. 120, 91 (1960).
- [14] S. V. Grigoriev, D. Chernyshov, V. A. Dyadkin, V. Dmitriev, S. V. Maleyev, E. V. Moskvin, D. Menzel, J. Schoenes, and H. Eckerlebe, Phys. Rev. Lett. 102, 037204 (2009).
- [15] S. V. Grigoriev, D. Chernyshov, V. A. Dyadkin, V. Dmitriev, E. V. Moskvin, D. Lamago, Th. Wolf, D. Menzel, J. Schoenes, S. V. Maleyev, and H. Eckerlebe, Phys. Rev. B 81, 012408 (2010).
- [16] A. N. Bogdanov and U. K. Rößler, Phys. Rev. Lett. 87, 037203 (2001).
- [17] S. V. Grigoriev, D. Lott, Yu. O. Chetverikov, A. T. D. Grünwald, R. C. C. Ward, and A. Schreyer, Phys. Rev. B 81, 195432 (2010).
- [18] J. M. Hopkinson and H.-Y. Kee, Phys. Rev. B 79, 014421 (2009).
- [19] L. Shekhtman, O. Entin-Wohlman, and A. Aharony, Phys. Rev. Lett. 69, 836 (1992).
- [20] T. Yildirim, A. B. Harris, A. Aharony, and O. Entin-Wohlman, Phys. Rev. B 52, 10 239 (1995).
- [21] International Tables for Crystallography, Vol. A: Space-Group Symmetry, T. Hahn (ed.). 1989. Kluwer Academic Publishers, Dordrecht, The Netherlands.
- [22] S. V. Grigoriev, S. V. Maleyev, A. I. Okorokov, Yu. O. Chetverikov, and H. Eckerlebe, Phys. Rev. B 73, 224440 (2006).
- [23] V. E. Dmitrienko, V. A. Chizhikov (unpublished).
- [24] F. Keffer, Phys. Rev. 126, 896 (1962).
- [25] L. Shekhtman, A. Aharony, and O. Entin-Wohlman, Phys. Rev. B 47, 174 (1993).
- [26] V. V. Mazurenko and V. I. Anisimov, Phys. Rev. B 71, 184434 (2005).
- [27] M. I. Katsnelson, Y. O. Kvashnin, V. V. Mazurenko, and A. I. Lichtenstein, Phys. Rev. B 82, 100403 (2010).

# ${\bf Tables}$

| n  | $\mathbf{r}_{ij}$                                   | t(i) | t(j) | $\mathbf{D}_{ij}$   |
|----|---|------|------|---------------------|
| 1  | $(-2x, \frac{1}{2}, \frac{1}{2} - 2x)$              | 1    | 2    | $(D_x, D_y, D_z)$   |
| 2  | $\left(\frac{1}{2} - 2x, -2x, \frac{1}{2}\right)$   | 1    | 3    | $(D_z, D_x, D_y)$   |
| 3  | $(\frac{1}{2}, \frac{1}{2} - 2x, -2x)$              | 1    | 4    | $(D_y, D_z, D_x)$   |
| 4  | $(2x, \frac{1}{2}, -\frac{1}{2} + 2x)$              | 2    | 1    | $(-D_x, D_y, -D_z)$ |
| 5  | $\left(-\frac{1}{2}, \frac{1}{2} - 2x, 2x\right)$   | 2    | 3    | $(-D_y, D_z, -D_x)$ |
| 6  | $\left(-\frac{1}{2} + 2x, -2x, -\frac{1}{2}\right)$ | 2    | 4    | $(-D_z, D_x, -D_y)$ |
| 7  | $\left(-\frac{1}{2} + 2x, 2x, \frac{1}{2}\right)$   | 3    | 1    | $(-D_z, -D_x, D_y)$ |
| 8  | $\left(-\frac{1}{2}, -\frac{1}{2} + 2x, -2x\right)$ | 3    | 2    | $(-D_y, -D_z, D_x)$ |
| 9  | $(2x, -\frac{1}{2}, \frac{1}{2} - 2x)$              | 3    | 4    | $(-D_x, -D_y, D_z)$ |
| 10 | $(\frac{1}{2}, -\frac{1}{2} + 2x, 2x)$              | 4    | 1    | $(D_y, -D_z, -D_x)$ |
| 11 | $(\frac{1}{2} - 2x, 2x, -\frac{1}{2})$              | 4    | 2    | $(D_z, -D_x, -D_y)$ |
| 12 | $(-2x, -\frac{1}{2}, -\frac{1}{2} + 2x)$            | 4    | 3    | $(D_x, -D_y, -D_z)$ |

TABLE I: The bonds between neighboring Mn atoms in MnSi crystal and corresponding Dzyaloshinskii–Moriya vectors. The listed 12 bonds are connected by symmetry transformations of the point group 23. Other 12 bonds appear owing to permutation of *i*-th and *j*-th atoms ( $\mathbf{r}_{ji} = -\mathbf{r}_{ij}$ ,  $\mathbf{D}_{ji} = -\mathbf{D}_{ij}$ ).

## **Figures**

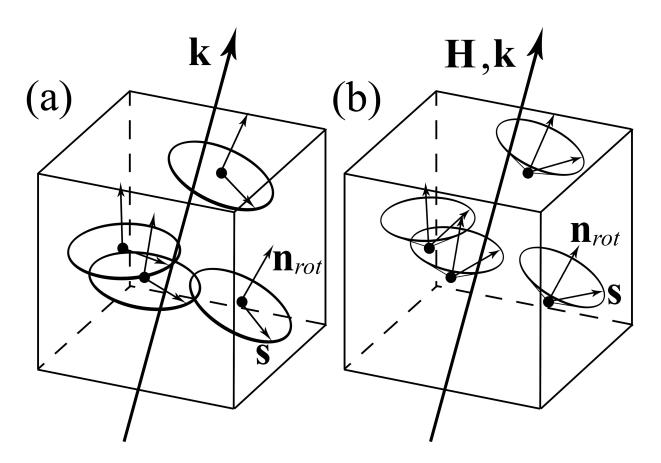


FIG. 1: (a) Organization of a free helix with an arbitrary wave vector  $\mathbf{k}$  (no magnetic field). The spins of each of four sublattices rotate around their own rotation directions  $\mathbf{n}_{rot}$  (see Eq. (30)), which differ slightly from that of  $\mathbf{k}$ . In the considered model, the energy of the free helix does not depend on direction of  $\mathbf{k}$  whereas experimentally the free helix is oriented either along [111] or [001] direction owing to the crystal field anisotropy. (b) Conical helix spin structure in an external magnetic field. The spins of each of four sublattices have a component directed along corresponding vector  $\mathbf{n}_{rot}$ ; its value is proportional to  $|\mathbf{H}|/H_c$  for  $|\mathbf{H}| \leq H_c$  and is equal to 1 for  $|\mathbf{H}| \geq H_c$ ;  $\mathbf{k}$ -vector is directed along the magnetic field.

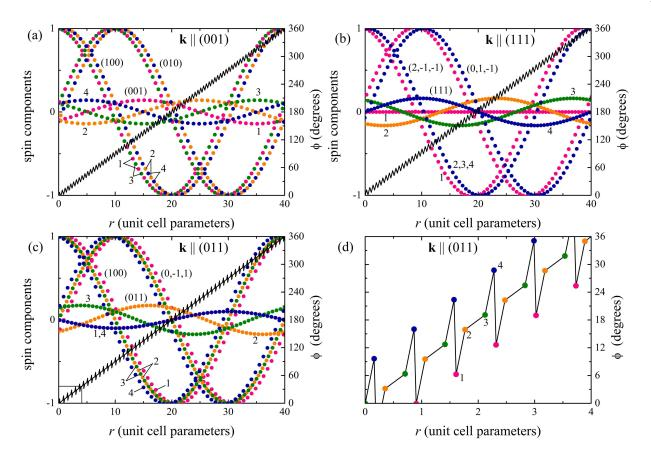


FIG. 2: (a)-(c) Details of spin helix structures calculated with the use of Eq. (31) for the wave vectors  $\mathbf{k}$  directed along (001), (111) and (011) crystal axes, correspondingly. The wave number  $|\mathbf{k}|$  is chosen to be equal to  $2\pi/40$ , which is close to the experimental value for MnSi crystal where the helix period is approximately 40 unit cells. The canting **D**-vector component is taken to be rather large,  $D_x + D_z = 0.4J$ , to emphasize nonmonotonic frustrated behavior of helices. Three spin components along directions  $\mathbf{n}_1$ ,  $\mathbf{n}_2$  and  $\mathbf{n}_3 = \mathbf{n}_k$  are presented by points with four colors corresponding to four sublattices. The black saw represents the angle  $\phi$  between spins in the successive ferromagnetic planes,  $\tan \phi = (\mathbf{s} \cdot \mathbf{n}_2)/(\mathbf{s} \cdot \mathbf{n}_1)$ . (d) An enlarged part of the saw restricted by a small box in (c); the line is drown to guide the eyes.